Optical monitoring of sweat pH by textile fabric wearable sensor based on covalently bonded Litmus-3-glycidoxypropyltrimethoxysilane coating

Michele Caldara, Claudio Colleoni, Emanuela Guido, Valerio Re, Giuseppe Rosace

University of Bergamo, Department of Engineering and Applied Sciences, Viale Marconi 5, 20244 Dalmine (Bg), Italy

Keywords: Litmus dye, Sol-gel, pH sensors, Optoelectronic read out, Wearable sensor.

Abstract

A wearable, flexible and non-toxic pH sensor was realized by assembling a cotton fabric treated with an organically modified silicate (ORMOSIL) together with a miniaturized and low-power electronics with wireless interface. The pH sensible ORMOSIL was obtained via sol–gel by using Litmus, a non-toxic pH indicator, and 3-glycidoxypropyltrimethoxysilane (GPTMS) as siloxane precursor. The chemical structure of the ORMOSIL was analyzed by FTIR and UV–vis spectroscopy. The electronics has been first characterized in a standalone fashion, and successively it has been coupled with the smart fabric, in laboratory and in preliminary on-body trials. The system is aimed to estimate indirectly the sodium (Na^+) concentration measured by the sweat pH. A sweat real-time monitoring is particularly attractive for healthcare, fitness and wellness areas.

1. Introduction

Recent developments in the field of nanotechnology [1,2] are of considerable interest in various academic and practical applications. Moreover, the integration of chemical sensing into textiles adds a new dimension to the field of smart clothing. In fact, pH-sensitive dye-doped mesostructured compounds are currently attracting interest in the textile field with respect to possible applications

for the detection of acidic or alkaline values for diagnostic as well as monitoring applications. This makes it possible to design an example of wearable sensor systems, including physiological and biochemical sensing, as well as motion sensing. Wearable chemical sensors may be used to provide valuable information about the wearer's health, monitoring the wearer during their daily routine within their natural environment. Sweat is a biofluid, mainly composed by water (99%), containing electrolytes and numerous other elements as urea, pyruvate and lactate [3,4]. Sweat loss from the whole total body vary between 300-700 mL/day [3] to the amount of 1.4 L/hour during prolonged exercise in the heat. As primary sweat electrolytes are concerned, sodium, chloride, potassium and calcium are present; among those, sodium (Na^+) has the highest concentration with a typical value of 38 mmol/L [5]. Perspiration is the main process to reduce body internal temperature increase due to physical exercise, but it is also generated in hot/humid environments and in presence of stress or emotion events.

A well-known technique for sweat analysis is the so-called whole body wash down, consisting in collecting all the body sweat for a subsequent analysis and weighting the subject. Patterson et al. [5] demonstrated that Na^+ total body concentration can be represented by samples collected in specific zones (lower-back, forearm, thigh, calf and foot) and that there is a positive relationship between sweat pH and sodium concentration, i.e. the greater the sodium levels, the higher the measured pH. Moreover it has also been observed that sweat pH rises in response to an increased sweat rate (SR) [6]. Thus, the sweat pH carries an information relevant to the body hydration level, which is very important in medicine for some pathology studies, but also in the fitness and wellness fields or for first-responders applications. Indeed, the body wash down technique is an highly desirable feature for optimal physiological balance, as the most recent commercial solutions for Cystic Fibrosis diagnosis [3] are not suitable for sweat continuous monitoring,. In recent years, some important work has been conducted in the real-time monitoring of human sweat with wearable detectors; focusing on colorimetric and electrochemical sensors. The latter can be further classified into the fabric/flexible plastic-based and epidermal-based sensors [7]. Colorimetric sweat analysis is one of

the most adopted techniques for CF diagnosis [3]. Curto et al. [8] focused their research on a microfluidic disposable patch, able to drive the sweat on a halochromic sensing area. Salvo et al. [9] conducted a study on measuring sweat rate exploiting humidity sensors, while Amay et al. exploited a potentiometric principle [10]. Rose et al. developed a patch that, using again a potentiometric approach, includes an RFID interface [11].

The aim of this work is to present the wearable application of a smart textile, made sensitive to pH with a non-toxic pH colorimetric molecule, combined with a miniaturized, low-power and high sensitivity electronics capable to monitor the fabric color and thus indirectly the pH. Depending on the mechanical set-up of the fabric, the sensor can monitor sweat pH or, alternatively, the environmental pH. Optical pH sensors offer several advantages with respect to classical electro-chemical pH electrodes, since they do not suffer from electromagnetic interference and thus their SNR is higher. Moreover, they present longer lifetime, reversible and fast responses, durability, low-cost, safety, ease of miniaturization and mechanical robustness. Thanks to these properties, applied to a comfortable substrate as the textile, this appears to be a very interesting solutions in view of integration in real garments. The functionalized fabric is the result of a sol–gel process; such technology makes it possible to incorporate a large number of organic and inorganic additives during the glass formation. In this way a big variety of studies and applications are viable. Several properties of sol–gel derived materials, most notably, those that are silica-based, make them particularly compatible with sensor development. The attractive points of sol–gel glasses are their ease of processability as well as their thermal and mechanical robustness. In the textile field they are regularly used to induce self-cleaning [12], hydrophobicity [13], flame retardant [14], antibacterial properties [15] or to immobilize dyestuffs on textile fabrics [16]. Moreover, sol–gel matrix is transparent in the UV and visible spectral range, making them amenable to common detection techniques such as absorption and reflection.

When the sol–gel technology is applied to obtain pH sensing performance, the diffusion of the molecules into the dried glass is sometimes a limiting factor, usually leading to rather long response

times (up to minutes). In this work, we show that mesoporous thin films, prepared by acidic sol–gel chemistry and low-temperature block-copolymer extraction, can function very effectively as pH sensors. The pH sensitive dye is covalently anchored to the mesoporous SiO_2 matrix in order to prevent leaching during optical pH measurements. We also demonstrate that the response of the dye-modified mesoporous silica thin films is very fast, indicating the possibility of using these materials in sensor devices.

The feasibility of introducing functional molecules into a 3-glycidoxypropyltrimethoxysilane (GPTMS) sol–gel matrix and the durability of their effect, also after immobilization onto textile fabrics, have been recently demonstrated in our previous work [17,18,19]. The developed halochromic textile retains not only the properties of other solid-state halochromic sensors, such as reversibility and harmlessness to the tested samples, but also some advantageous features, such as simple fabrication, durability and wearability. Particularly, changes can be monitored in the reflectance intensity associated with the protonation–deprotonation process on dedicated instrumentation attached to the halochromic fabric.

The entrapment of halochromic molecules into hybrid sol–gel matrices considerably affects their protonation equilibria and thus changes their pKa values [17,18]. The shift of pKa values is often related to the chemical structure of the indicator and the nature of the sol–gel precursors used. In order to obtain matrices with suitable properties for use in sensing applications, including appropriate surface polarity, mechanical stability, porosity, thickness, and uniformity, the free litmus is covalently bonded to the silica precursor. The litmus-silica was obtained by a sol–gel process through the functionalization of reactive groups present in the aromatic ring of the chromophore with 3-glycidoxypropyltrimethoxysilane in water solution, in a one-pot reaction. The effects of film processing parameters and the effects of organic modification of the silica matrix on the visible spectral properties and analytical performance of the entrapped indicators were determined. The potential for further development of these films as optical sensors and biosensors is discussed.

2. Experimental part

2.1. Material and methods

Scoured and bleached 100% plain-weave cotton fabric (weight 237 g/m^2) was used in this work. The fabrics were cleaned before treatment by washing in 2% non-ionic detergent at pH 7 and 40°C for 20 min, and then rinsed several times with de-ionized water, dried and put into a drier for storage. Prior to all experiments, the samples were conditioned under standard atmospheric pressure at 65 ± 4% relative humidity and 20 ± 2°C for 24 h.

7-hydroxyphenoxazone (Litmus), GPTMS, BF_3OEt_2, Na_2HPO_4/Citric Acid buffers (A.R. grade) and other chemicals were purchased from Aldrich and used as received.

The pH dependence of the measurements was evaluated by using eight different pH values, obtained by McIlvaine Na_2HPO_4/citric acid buffers [20].

As reported by Beecken et al. [21], the principal constituent of litmus is a 7-hydroxyphenoxazone chromophore. In acidic solution it combines with a proton to yield the red cation HL^+, and in basic solutions it eliminates a proton to give the blue L^- species, as shown in Fig. 1. The color changes are performed in the pH range 4.5–8.3.

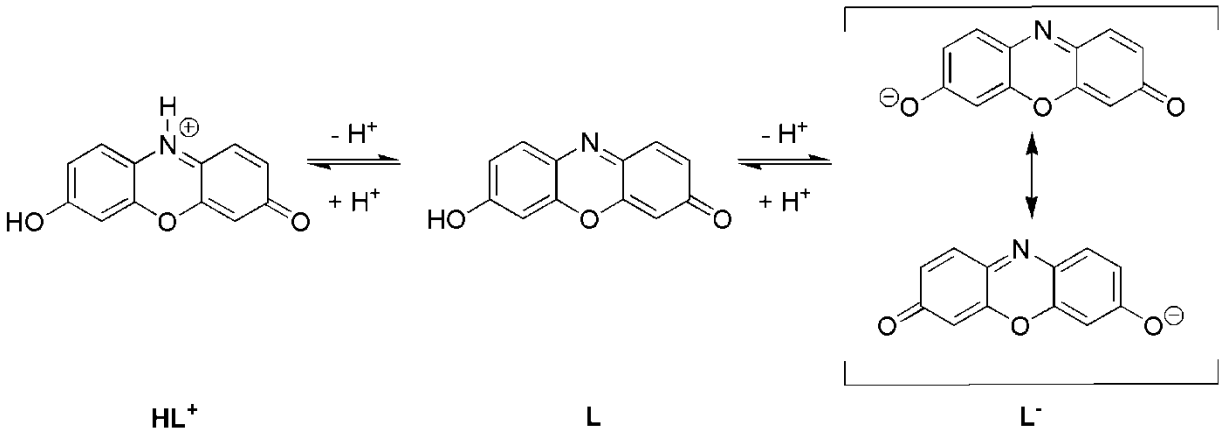

Fig. 1. Acid (HL^+), neutral (L) and basic (L^-) forms of Litmus molecule.

Litmus was involved as nontoxic halochromic reactive dye in the presence of the GPTMS precursor

and the BF_3OEt_2 epoxy ring opening catalyst, by applying a modification of the synthesis method already published [19].

The hybrid sol was synthesized by adding GPTMS (0.3 M, 10:1 molar ratio with respect to litmus) to a water solution of litmus in the presence of a catalytic amount of BF_3OEt_2 (10% w/w GPTMS) and stirred for 4 h at reflux conditions. After this time, NaOH was added (4% of a 2 M solution) to obtain a final pH value of 4. The filtered solution was fully characterized by UV–vis spectroscopy, in buffered solutions at different pH values, and by FT-IR spectroscopy, as solid residue. The cotton fabrics (20 cm x 30 cm) were impregnated with the GPTMS-litmus sol and, afterward, were passed three times through a two-roll laboratory padder (Werner Mathis, Zurich, Switzerland) at nip pressure of 3, with 75% of wet pick-up. Then, the treated samples were dried at 80°C for 30 min and were cured at 170°C for 5 min. For comparison, cotton samples, dyed with litmus only, were prepared in the same way. All specimens were characterized by FT-IR spectroscopy. To evaluate washing resistance, cotton fabrics were washed with 1 washing cycle, according to the international standard EN ISO 6330:2000 [22], in a Labomat Mathis equipment (Werner Mathis AG).

2.2. Measurements and analysis

FT-IR spectra were recorded with a Thermo Avatar 370, equipped with attenuated total reflection (ATR) accessory. A Diamond crystal was used as internal reflectance element on the ATR accessory. Spectra were acquired, at room temperature, in the range from 4000 to 550 cm^{-1}, with 32 scans and a resolution of 4 cm^{-1}. UV–vis measurements were performed with a Thermo Nicolet Evolution UV-vis-500 spectrophotometer, using a 1 cm pathlength cell. All spectra were acquired at room temperature.

UV–vis measurements were performed with a Thermo Nicolet EvolutionUV-vis-500 spectrophotometer. For the absorption spectra of solutions, 1 cm matched quartz cells were used. All spectra were acquired at room temperature.

2.3. System Layout

The smart fabric has been coupled to a multi-sensor platform, having external dimensions of only 50 mm x 47 mm x 15 mm (Fig. 2). The electronics includes a color sensor, a skin thermometer, embedded processing devices and a Bluetooth radio. As schematized in Fig. 2, the laboratory characterizations and the preliminary on-body trials were conducted placing a white cotton fabric between the functionalized textile and the skin, in order to minimize the skin color influence on the fabric. Due to the slow variation of sweat composition, the measurements are performed every 5 seconds. A PC based software has been developed for measurement control and continuous data upload. Sweat pH was measured locally five times during the trial on the exercise bike with a reference portable pH-meter (Hanna Instruments Skincheck), with a precision of 0.01 pH after calibration with standard buffer solutions.

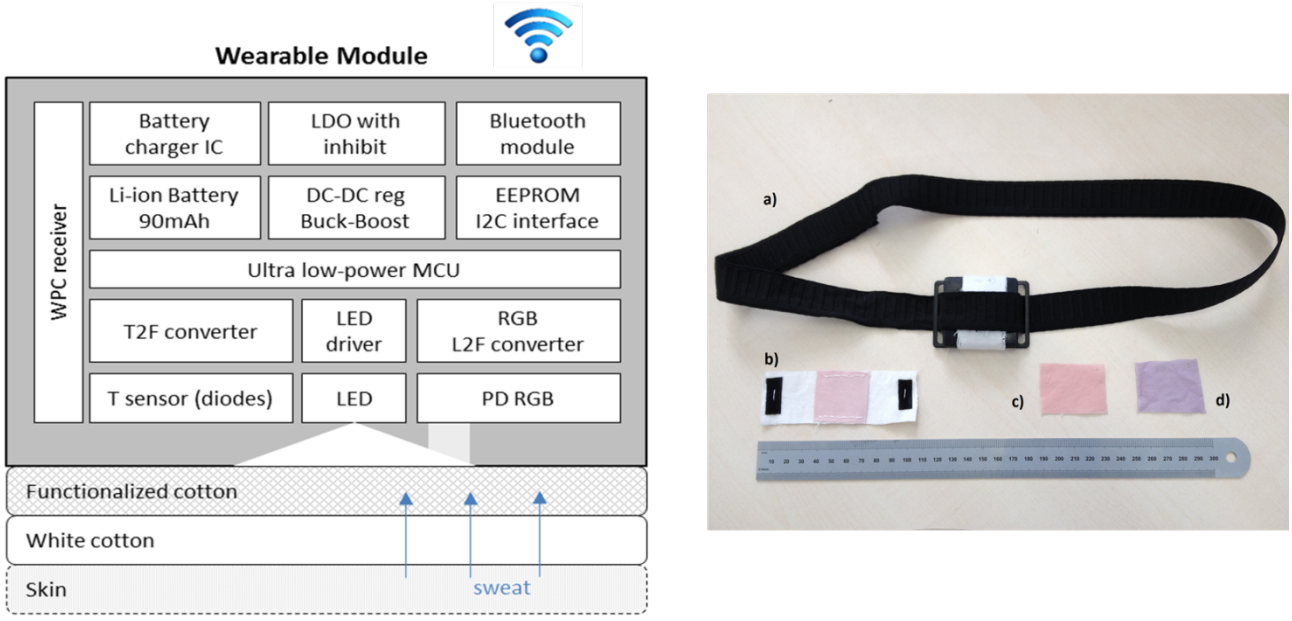

Fig. 2. Block diagram of the wearable system, where the main components are shown (left); photograph of the system (right), where a) is the electronics coupled with the textile patch and an elastic bend for trunk mounting, b) is the textile assembly, where the smart fabric is attached to a white cotton, c) and d) are two samples of smart fabric wet respectively with buffer solutions at pH 5 and pH 8.

2.4. Optical detection

The state-of-the art color/light sensors (see Table 1) integrate a photodiode (PD) or a matrix of PDs and the processing electronics in the same package, providing a digital output on different protocols; despite the compactness and the performance of such devices, considering their general high power consumption, the high price and the lack of flexibility in choosing a suitable PD, a dedicated readout was developed. The fabric color is detected using an optoelectronic circuit placed in front of it, working in a reflective way. The system, enclosed into a black box except for the viewing port, is mainly composed by a high luminosity white LED (Vishay VLMW41S1T1), controlled by a dedicated driver in order to maintain constant illumination and an RGB photodiode (Hamamatsu S90032-02), placed as close as possible to the LED in order to collect the maximum reflected light from the fabric. The photocurrent from each of the three colors is converted into a pulse train by means of a light to frequency (L2F) circuit, whose principle is described in a previous paper [23].

Pivotal advantages arise in connecting a PD in a L2F circuit; first, there is no need of amplification, because of the high sensitivity (typically 205 Hz/lux). Second, there is no need to introduce filtering techniques, since the photocurrent integration on a capacitor through a resistor is a low-pass filter (fLP=1.6kHz with the actual values). Furthermore, there is no need to manage saturation thanks to the extended dynamic range of the circuit (40dB with the chosen values) and the power consumption is only 0.71mW (255μA with VDD 2.8V). Finally, the quasi-digital output, that is a pulse train with a frequency proportional to the photocurrent magnitude, makes it possible to avoid using an ADC. Signal acquisition has been implemented with a direct connection to microcontroller timer peripherals; two methods have been compared. The first one is based on counting the rising edges of the L2F output signals in a fixed time interval (1s in this study, implying 1Hz reading resolution, corresponding to 1nA PD current variation); the longer the time interval, the higher the accuracy and sensitivity of the frequency measure. The second method involves the logic high time

interval, in such a way to minimize the measuring time needed to obtain a reliable measurement. Such single period measurement simply counts the microcontroller clock periods using the input signal as a gate. The microcontroller used in this sensor platform is STM8L151C6, which is particularly suitable for wearable applications thanks to its extremely low power consumption of 180 μA/MHz in run mode. By applying the L2F principle to an RGB readout, the system is capable to detect any color in the visible spectrum, representing a flexible readout system for studying textiles, functionalized with different colorimetric dyes.

Table 1

Main features of state-of-the-art color sensors

Vendor/Model	Type	Output	Sensitivity Light condition	Sensitivity				Power supply	
				Data			Unit	I_{DD} [mA]	V_{DD} [V]
Hamamatsu S9706	RGB	Serial custom	G	R: 5.8	G: 4.1	B: 1.9	LSB/lux	5÷10	3÷5.5
Taos TCS3472	RGB+VIS	I2C	R/G/B	R: 18.5	G: 12.0	B: 9.3	counts/μW/cm^2	235÷330 e^{-3}	2.7÷3.3
Taos TCS3200	RGB+VIS, L2F	Pulse Train	R/G/B	R: 448	G: 264	B: 240	Hz/μW/cm^2	1.4÷2	2.7÷5.5
Taos TSL2581	VIS+IR	I2C	λ_{peak} 625nm	VIS: 29.1		IR: 4	counts/μW/cm^2	175÷250 e^{-3}	2.7÷3.6
Taos TSL2572	VIS+IR	I2C	White	VIS: 18.9		IR: 2.58	counts/μW/cm^2	200÷250 e^{-3}	2.7÷3.6
Hamamatsu S9705	VIS, L2F	Pulse Train	2856K		500		Hz/lux	1.5÷3	2.7÷5.5
Avago APDS-9303	VIS+IR	I2C	λ_{peak} 640nm		27.5		counts/μW/cm^2	0.24÷0.6	2.7÷3.6
Proposed RGB L2F Color sensor	**RGB, L2F**	**Pulse Train**	**White, avg fabric color**		**205**		**Hz/lux**	**255 e^{-3}**	**2.8**

RGB= red/green/blue, VIS= visible light, IR=Infrared light

Sensitivity values refer to a particular illumination condition which is different between devices.

3. Results and discussion

3.1. FT-IR characterization

The analysis of pure xerogels were performed on optical quality glass slides, since the infrared absorption bands characteristics of the thin films applied onto the fabric surface are overlapped by the strong vibrational modes of cellulose falling in the same spectral range. Fig. 3 compares the FT-IR spectra acquired for pure litmus, GPTMS sol and for GPTMS-litmus sol as solid residue. Pure litmus shows several peaks at 3290, 1730, 1650, and 1454 cm^{-1}, which can be assigned to O–H, C=O, C=C and C=N, and C–C bonds, respectively. In the FT-IR spectrum of the GPTMS xerogel, the broad absorption between 3700 and 3100 cm^{-1} is due to the –OH stretching vibrations. The epoxy-ring is identified by the characteristic absorption bands at 3057 cm^{-1} (asymmetric C–H stretch in the epoxy), 2999 cm^{-1} (symmetric C–H stretch in the epoxy), 1255 cm^{-1} (ring breathing), 907 cm^{-1} (asymmetric ring deformation), and 851 cm^{-1} (symmetric ring deformation). The ether linkages in the glycidoxy group are overlapped by the strong Si–O–Si absorption at 1090 cm^{-1}. Furthermore, the symmetric Si–O–Si stretching vibrations can be seen at around 800 cm^{-1}. The stretching of –CH groups is visible around 2940-2860 cm^{-1} and the corresponding bending vibrations can be seen around 1490 cm^{-1}. When GPTMS reacts with Litmus in the presence of BF_3, the absorption bands relative to the epoxy-ring disappear completely, as shown in Fig. 3.

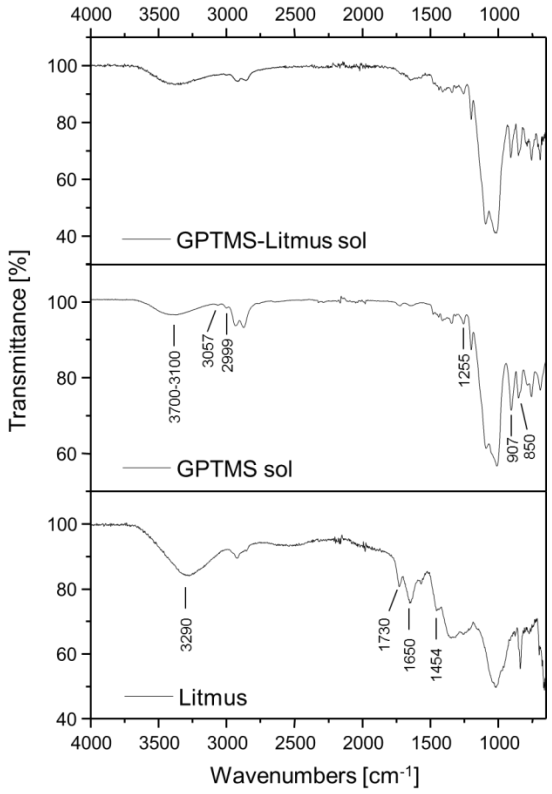

Fig. 3. FTIR spectra of Litmus, GPTMS sol, GPTMS-Litmus applied on glass-slides.

In the FTIR spectra of cotton treated with GPTMS-Litmus sol the presence of the SiO_2 matrix is confirmed by the Si–O–Si bending absorption at 875 cm^{-1} and the stretching absorption at 790 cm^{-1}.

3.2. UV-visible spectral characterization

The investigation of litmus behaviour in solution was carried out by UV–vis analysis. All spectra were acquired in buffered solutions in the range 400-800 nm by varying the pH value to evaluate his influence on the color change of litmus. The effect of the matrix (GPTMS sol) on the litmus absorption spectra was also studied. Fig. 4 shows the UV–vis absorbance spectra of free indicator and immobilized litmus solutions at pH 2 and 8, after normalization of the spectra to a value of 1 at the peak maximum. It is interesting to note that the immobilization of litmus with GPTMS via sol–gel does not lead to the loss of its pH response, but the spectrum of the immobilized litmus exhibits similar absorption bands as that of litmus solutions at acid pH values until pH=5. Starting by pH 6,

the response of the two samples with the pH change shows same differences, as reported in Fig. 4 at pH 8. In fact, the alkaline peak maximum showed a little red shift from 580 nm in the pure litmus solution to 584 nm in the GPTMS-litmus sol, with the formation of a very broad band respect to the pure litmus. This is probably due to the formation of a covalent bond between GPTMS and litmus.

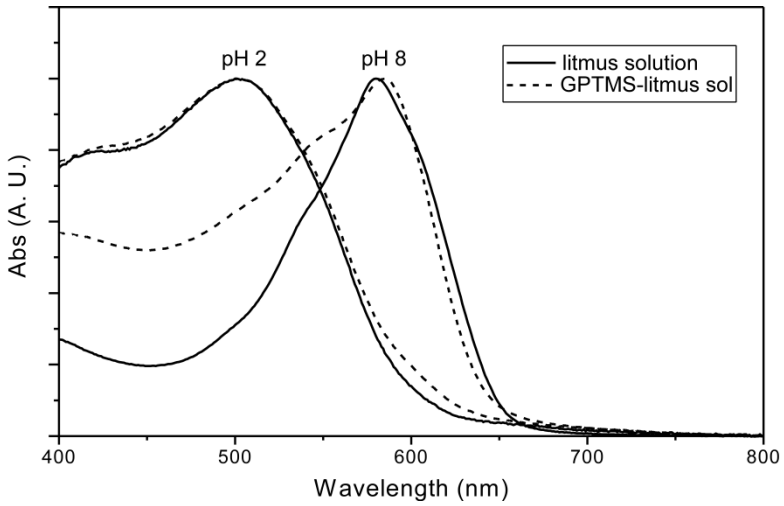

Fig. 4. Normalized UV–visible spectra of Litmus (solid line) and GPTMS-Litmus sol (dashed line) at pH 2 and 8.

3.3. System characterization

The electronics has been first characterized in a standalone fashion, in order to investigate its performance. Each component of the photodiode (Red (R), Green (G) and Blue(B)), generates, as L2F output, a frequency in the order of some hundreds of Hertz. The readout of such frequencies, placing the color sensor electronics over a fixed color for 10 minutes, has excellent stability: the measured standard deviation with respect to the mean readings was of 0.3%. As a second step, a dry fabric sample has been measured with the electronics in the configuration shown in Fig. 2 for about one hour, to confirm the system stability in a wearable scenario in which sweating occurs not immediately after the system is worn. The measured stability of the dry textile readings resulted to be comprised within 0.4% standard deviation with respect to the average acquired frequencies. Successively the system has been characterized by applying 0.13 ml of buffer solutions at different pH on 7 cm^2 fabric samples, placed under the electronics. Each specimen was first measured with a

reference pH-meter and successively a set of three measurements has been performed with our system, leading to the result summarized in Fig. 5. As expected, by applying alkaline solutions the Blue color contribution rises, while the Red and Green contributions decrease. By elaborating the data of Fig. 5, a predictive model for pH has been estimated, obtaining the results depicted in Fig. 6. Since from pH 3 to 4 the color variation is minimal, pH 3 was excluded from the regression model, obtaining an estimation error in determining the pH of the impregnated fabric within ±0.5 pH from pH 4 to more than 10. Moreover, since the green contribution total variation along the pH range is the lowest with respect to the Red and Blue one, a model not taking into account its contribution has been computed, obtaining comparable results with respect to the RGB model. This could be exploited for reducing further the power consumption of the system. For preparing the final wearable application, the fabric color settling time, once the sweat or the liquid wets the fabric, is fundamental. Fig. 7 shows that the color change, from a dry textile sample on which 0.13 ml were applied in 1 second, takes place in much less than 5 sec, which is the time granularity of the measurements. Immediately after application the color is settled within few percent of its final hue, which occurs about 110 seconds after. The immediate color change is substantial improvement in the fabric treatment, if compared with the results presented with Methyl Red dye in a previous work [17], where the color was smoothly changing for 180 seconds. In particular this fast reaction is attractive for future harmful gas/vapour sensing.

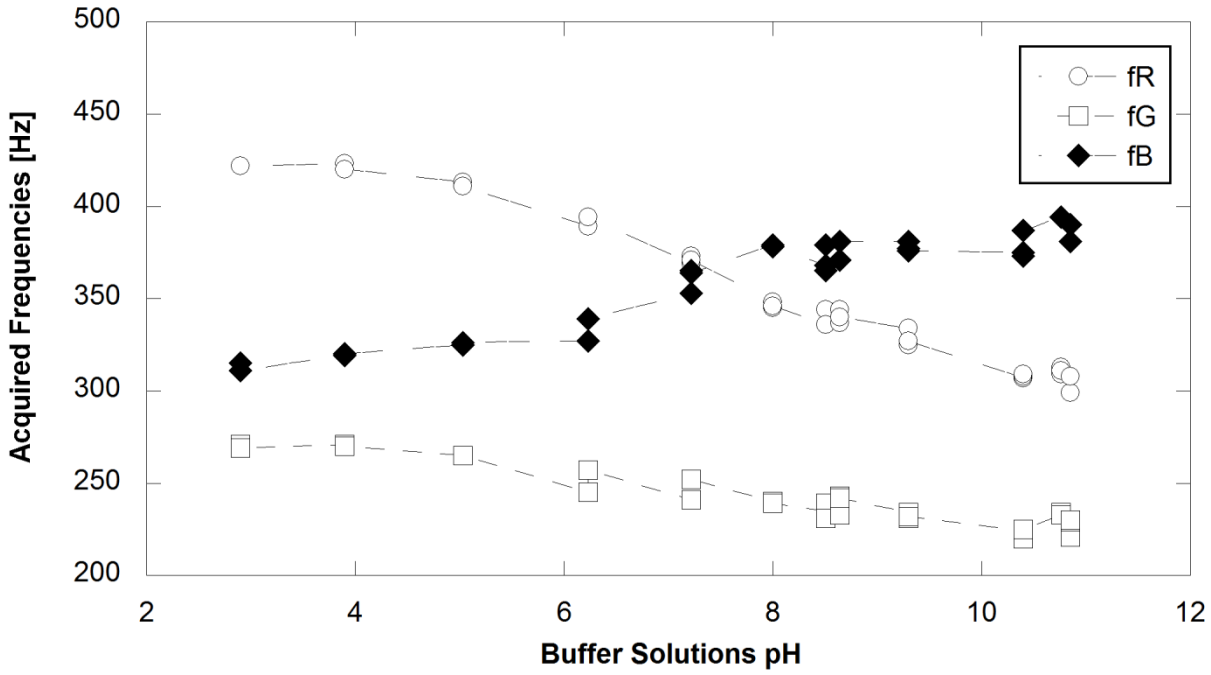

Fig. 5. Measurement on different fabric samples wet with different buffer solutions pH.

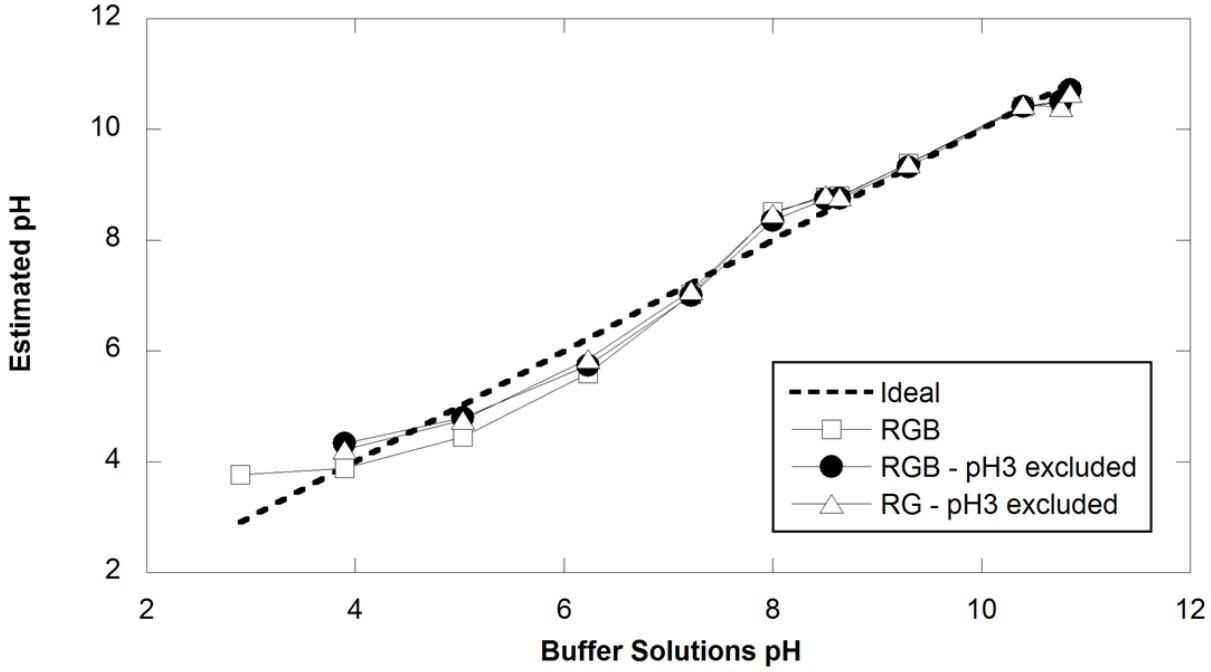

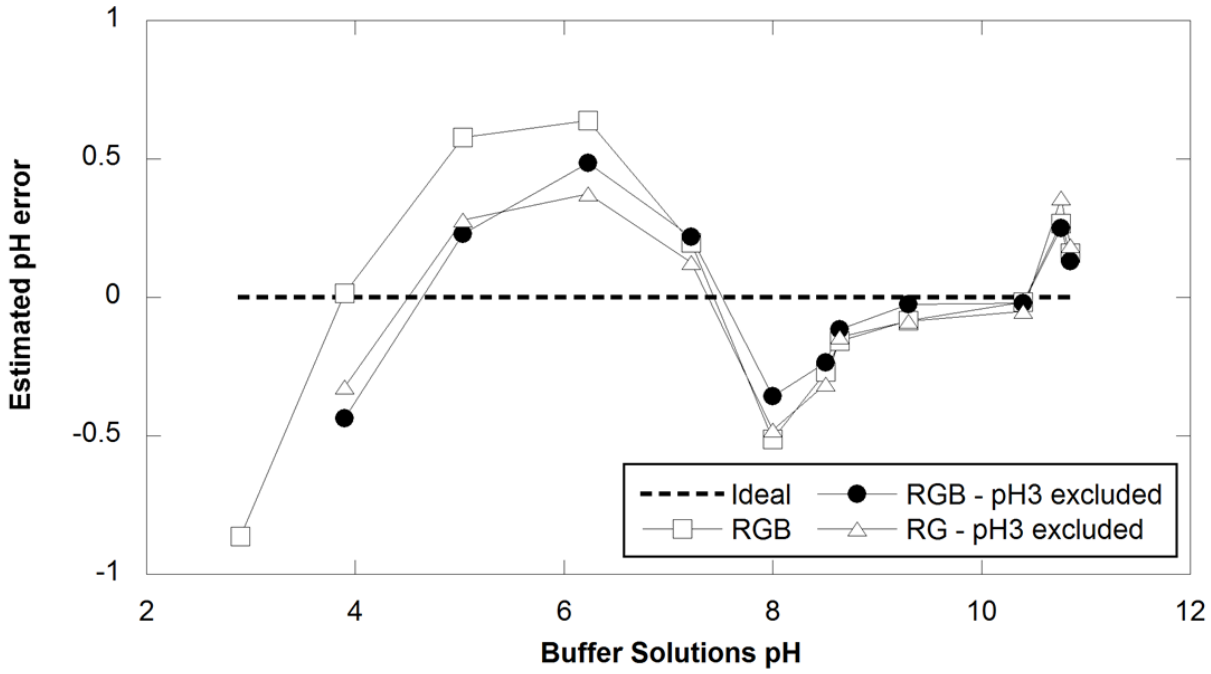

Fig. 6. Results on the pH estimation model; correspondence between reference and estimated pH (top) and the absolute error with respect to the reference pH (bottom).

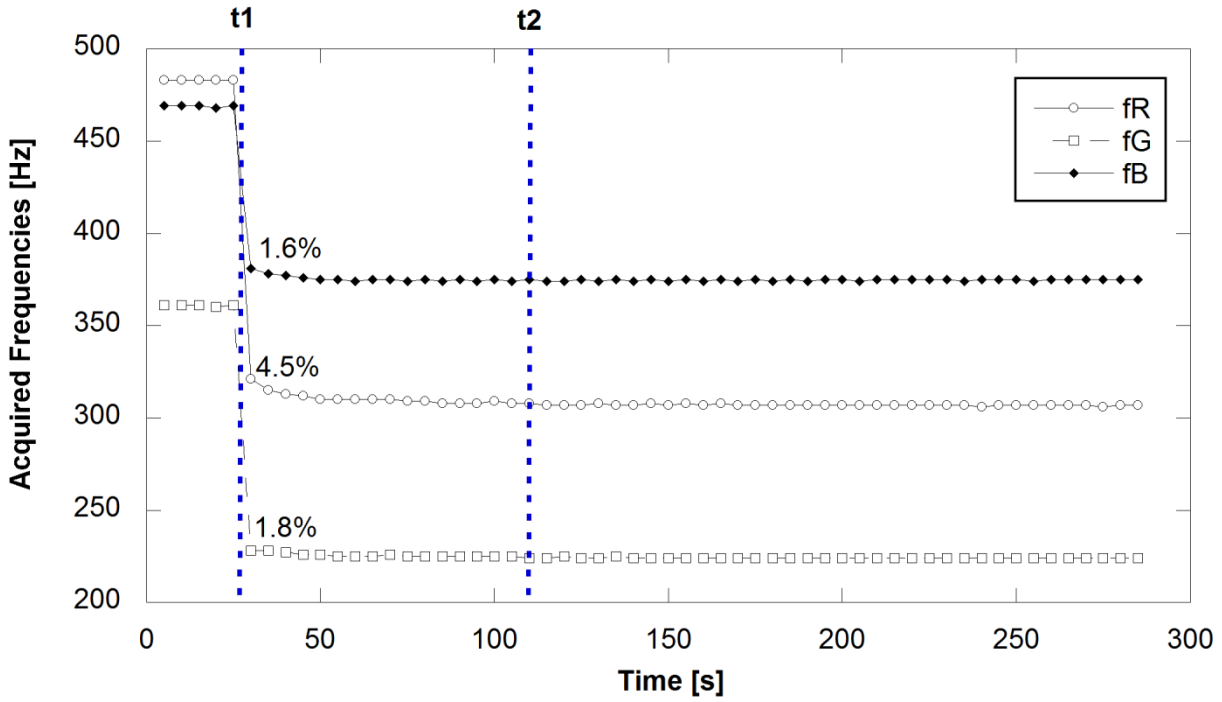

Fig. 7. System readings during the application (at second 27) of a pH 10.4 buffer solution on a dry fabric. The percentage indicates the deviation of the first reading after the buffer solution application from the stable final color. t1: buffer solution application; t2: textile color complete stabilization.

3.4. On-body trials

Sweat is a body fluid mainly produced by the eccrine sweat glands, distributed over nearly the entire body surface. Sweat is transported to the skin surface by means of secretory ducts. It is proved that, during heat stress or exercise, in order to improve body heat dissipation through evaporation, the skin sympathetic nerve activity generates sweating. During sweat expulsion in the duct, ions like sodium and chloride are reabsorbed. However, when sweat rate rise, reabsorption is overwhelmed, leading to an increase in ion losses [24]. Sweating is primarily controlled by central brain temperature and secondarily affected by mean skin temperature. During the initial phase of sweating, increases in sweating occur due to an increase in the number of active sweat glands and an increase in the volume of sweat produced by each gland. Most of the sweat glands are activated

within 8 minutes of exercise or passive exposure to heat. Afterwards, increases in the volume of sweat produced per gland occur gradually, until heat stress or exercise is withdrawn, or after prolonged heat stress (5–6 hours) when sweating reduces regardless of stimuli.

Skin pH is affected [25] by endogenous (e.g. age, ethnicity, sebum content, skin moisture) and exogenous factors, like cosmetics, detergents and occlusive dressings as well as topical antibiotics, so that the pH of each individual varies with respect to the others and, also, with respect to itself during the day. Variable skin pH values are being reported in literature, all in the acidic range but with a broad range from pH 4.0 to 7.0 [26].

A skin pH measurement campaign, at rest, on five volunteers during one month time, performed once a day randomly with a reference portable pH-meter, demonstrated a skin pH of 5±0.44. This preliminary result suggests that a sweat real-time monitoring must be tailored to each individual, depending on the basal pH of the skin. The developed system, as depicted in Fig. 2, was placed on the lumbar region of a subject during a physical activity session on an exercise bike; the choice of the lower back was driven by the results presented in [5], showing the most representative body region of the whole body, together with a possible future integration in a fitness shirt. The electronics and the textile were adherent to the skin thanks to an elastic strap, thus ensuring an effective sweat collection and a good shielding from ambient light. Sweat pH was measured locally five times during the trial on the exercise bike with a reference pH-meter. The results are shown in Fig. 8. For the first 200 seconds, the signal does not change compared to the initial evaluation at t_0, due to the low sweating during physical activity that is not enough for wetting the fabric sensor. After that the textile changes lightly its color in the first 1100 seconds due to the limited sweat rate [27] useful to wet slowly the cotton fabric. Whereupon this first settling interval of training period the difference in measurements by this method, with respect to a reference glass pH meter, was found to be less to 0.5 of a pH unit. Therefore, the pH of the sol-gel based wearable sensor fits reasonably well with the commercial pH probe reference measurements. Moreover the pH readings resolution is of 0.2 pH unit, which can be further reduced with averaging, due to the slow process of

pH change. The obtained result is in accordance with what reported in literature, in particular for the pH value and its variations [8,28,29].

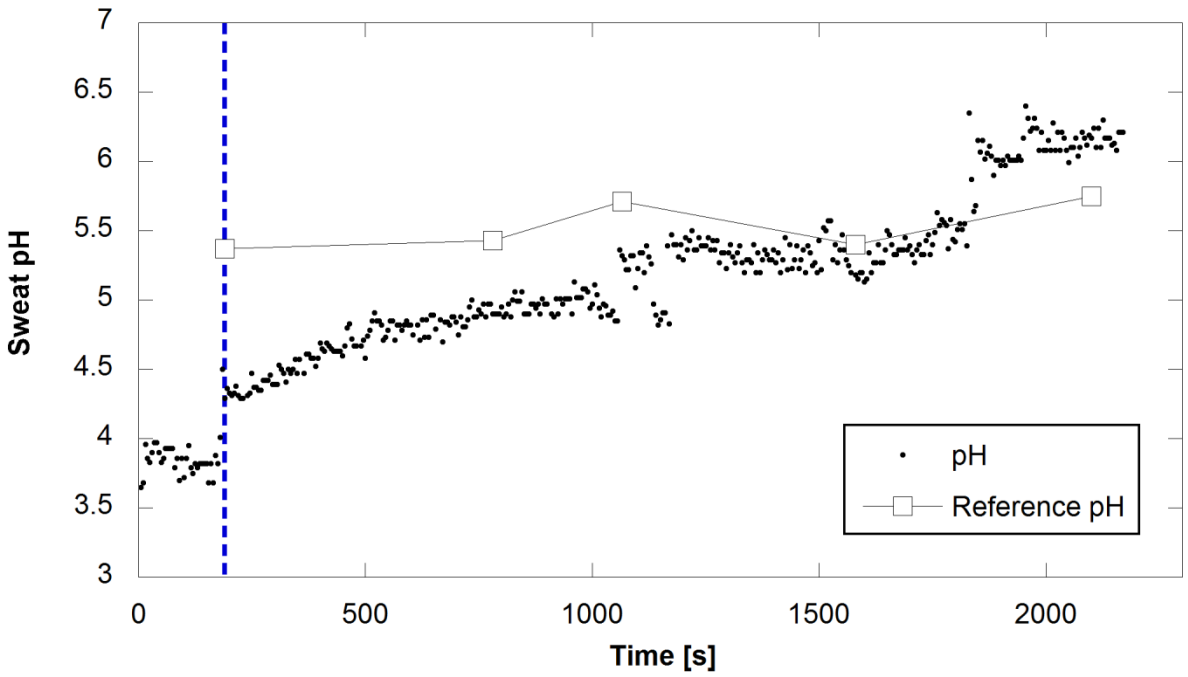

Fig. 8. On-body measurement during physical activity on the exercise bike. A dotted vertical line shows the perspiration process start.

Conclusion

This paper presented the development of a wearable platform, used in conjunction with a smart textile, able to continuously measure the pH of the sweat. The technologies adopted for both smart textile fabrication and the wearable electronics were presented. The smart fabric has been obtained via sol–gel using an environmental friendly halochromic dye, i.e. Litmus. The electronics features a low-power, high sensitivity color sensor, embedded processing and Bluetooth interface. The system has been first characterized in the laboratory using buffer solutions in a pH range compatible with sweat variations, in order to get a pH estimation model. The module was finally used in an exercise bike session, obtaining a settling time of 8 minutes, partially due to the limited sweat rate of the

beginning of perspiration, a 0.2 pH resolution and accordance with respect to a reference electro-chemical pH-meter within 0.5 pH. A main goal of this system is indeed the non-invasive estimation of the body hydration level, whose study is presently in progress. Such a textile-based continuous monitoring sweat sensor could provide a new tool, not only in the fitness field, but also in the medical research field, for disease diagnosis and drug assumption monitoring.

References

[1] B. Mahltig, T. Textor, Nanosols and Textiles, first ed., World Scientific, London, 2008.
[2] E. Guido, J. Alongi, C. Colleoni, A. Di Blasio, F. Carosio, M. Verelst, G. Malucelli, G. Rosace, Thermal stability and flame retardancy of polyester fabrics sol-gel treated in the presence of boehmite nanoparticles , Polym. Degrad. Stabil. 98 (2013) 1609–1616.
[3] A. Mena-Bravo, M. D. Luque de Castro, Sweat: A sample with limited present applications and promising future in metabolomics, J. Pharm. Biomed. Anal. 90 (2014) 139–147.
[4] C. J. Harvey, R. F. LeBouf, A. B. Stefaniak, Formulation and stability of a novel artificial human sweat under conditions of storage and use, Toxicol. in Vitro 24 (2010) 1790–1796.
[5] M. J. Patterson, S. D. R. Galloway, M. A. Nimmo, Variations in Regional Sweat Composition in Normal Human Males, Exp. Physiol. 85 (2000) 869–875.
[6] R. M. Morgan, M. J. Patterson, M. A. Nimmo, Acute effects of dehydration on sweat composition in men during prolonged exercise in the heat, Acta Physiol. Scand. 182 (2004) 37–43.
[7] A. J. Bandodkar, J. Wang, Non-invasive wearable electrochemical sensors: a review, Trends Biotechnol. 32 (2014) 363–371.
[8] V. F. Curto, C. Fay, S. Coyle, R. Byrne, C. O'Toole, C. Barry, S. Hughes, N. Moyna, D. Diamond, F. Benito-Lopez, Real-time sweat pH monitoring based on a wearable chemical barcode micro-fluidic platform incorporating ionic liquids, Sensors and Actuators B:Chemical 171–172 (2012) 1327–1334.
[9] P. Salvo, F. Di Francesco, D. Costanzo, C. Ferrari, M. G. Trivella, D. De Rossi, A Wearable Sensor for Measuring Sweat Rate, Sensors Journal, IEEE , 10 (2010) 1557–1558.
[10] A. J. Bandodkar, D. Molinnus, O. Mirza, T. Guinovart, J. R. Windmiller, G. Valdés-Ramírez, F. J. Andrade, M. J. Schöning, J. Wang, Epidermal tattoo potentiometric sodium sensors with wireless signal transduction for continuous non-invasive sweat monitoring, Biosens. Bioelectron. 54 (2014) 603–609.
[11] D. P. Rose, M. Ratterman, D. K. Griffin, L. Hou, N. Kelley-Loughnane, R. R. Naik, J. A. Hagen, I. Papautsky, J. Heikenfeld, Adhesive RFID Sensor Patch for Monitoring of Sweat Electrolytes, Biomedical Engineering, IEEE Transactions on, 99 (2013) 1–9 doi: 10.1109/TBME.2014.2369991.
[12] C. Colleoni, M.R. Massafra, G. Rosace, Photocatalytic properties and optical characterization of cotton fabric coated via sol-gel with non-crystalline TiO_2 modified with poly(ethylene glycol), Surf. Coat. Technol. 207 (2012) 79–88.
[13] C. Colleoni, E. Guido, V. Migani, G. Rosace, Hydrophobic behaviour of non-fluorinated sol–gel based cotton and polyester fabric coatings, J. Ind. Text. 44 (2015) 815–834.

[14] J. Alongi, C. Colleoni, G. Rosace, G. Malucelli, Phosphorus- and nitrogen-doped silica coatings for enhancing the flame retardancy of cotton: Synergisms or additive effects?, Polym. Degrad. Stabil. 98 (2013) 579–589.
[15] A. Farouk, S. Moussa, M. Ulbricht, E. Schollmeyer, T. Textor, ZnO-modified hybrid polymers as an antibacterial finish for textiles, Text. Res. J. 84 (2014) 40–51.
[16] B. Mahltig, H. Böttcher, D. Knittel, E. Schollmeyer, Light fading and wash fastness of dyed nanosol-coated textiles, Text. Res. J. 74 (2004) 521–527.
[17] M. Caldara, C. Colleoni, E. Guido, V. Re, G. Rosace, Development of a textile-optoelectronic pH meter based on hybrid xerogel doped with Methyl Red, Sensors and Actuators B:Chemical 171–172 (2012) 1013–1021.
[18] L. Van der Schueren, K. De Clerck, G. Brancatelli, G. Rosace, E. Van Damme, W. De Vos, Novel cellulose and polyamide halochromic textile sensors based on the encapsulation of Methyl Red into a sol–gel matrix, Sensors and Actuators B:Chemical 162 (2012) 27–34.
[19] E. Guido, C. Colleoni, K. De Clerck, M. R. Plutino, G. Rosace, Influence of catalyst in the synthesis of a cellulose-based sensor: Kinetic study of 3-glycidoxypropyltrimethoxysilane epoxy ring opening by Lewis acid, Sensors and Actuators B:Chemical 203 (2014) 213–222.
[20] A. Vogel, Textbook of Quantitative Inorganic Analysis, Longmans, London, 1944.
[21] H. Beecken, E.M. Gottschalk, U.v. Gizycki, H. Krämer, D. Maassen, H.-G. Matthies, H. Musso, C. Rathjen, U. I. Zdhorszky, Orcein and Litmus, Biotechnic. & Histochem. 78 (2003) 289–302.
[22] EN ISO 6330:2000, Textiles – Domestic Washing and Drying Procedures for Textile Testing.
[23] M. Caldara, C. Colleoni, E. Guido, G. Rosace, V. Re, A. Vitali, A wearable sensor platform to monitor sweat pH and skin temperature, Body Sensor Networks (BSN), 2013 IEEE International Conference on, vol., no., pp.1,6, 6-9 May 2013, doi: 10.1109/BSN.2013.6575465.
[24] M. Shibasaki, T.E. Wilson, C.G. Crandall, Neural control and mechanisms of eccrine sweating during heat stress and exercise, J Appl Physiol 100 (2006) 1692–1701.
[25] M.-H. Schmid-Wendtner, H.C. Korting, The pH of the Skin Surface and Its Impact on the Barrier Function, Skin Pharmacol Physiol 19 (2006) 296–302.
[26] H. Lambers, S. Piessens, A. Bloem, H. Pronk, P. Finkel, Natural skin surface pH is on average below 5, which is beneficial for its resident flora, Int J Cosmet Sci. 28 (2006) 359-70.
[27] D. Morris, S. Coyle, Y.Z. Wu, K.T. Lau, G. Wallace, D. Diamond, Bio-sensing textile based patch with integrated optical detection system for sweat monitoring, Sensors and Actuators B:Chemical 139 (1) (2009) 231–236.
[28] A. J. Bandodkar, V. W. Hung, W. Jia, G. Valdés-Ramírez, J. R. Windmiller, A. G. Martinez, J. Ramírez, G. Chan, K. Kerman, J. Wang, Tattoo-based potentiometric ion-selective sensors for epidermal pH monitoring, Analyst. 138 (2013) 123–128.
[29] V.F. Curto, C. Fay, S. Coyle, R. Byrne, C, O'Toole, C. barry, S. Hughes, N. Moyna, D. Diamond, F. Benito-Lopez, Real-timesweat pH monitoring based on a wearable chemical barcode micro-fluidicplatform incorporating ionic liquids, Sens. Actuators B: Chem. 171 (2012)1327–1334.